J. Phys. B: At. Mol. Opt. Phys. **42** (2009) 134012 (9pp) doi:10.1088/0953-4075/42/13/134012

EUV-photon-induced multiple ionization and fragmentation dynamics: from atoms to molecules

Y H Jiang[1], A Rudenko[2], M Kurka[1], K U Kühnel[1], L Foucar[3], Th Ergler[1], S Lüdemann[1], K Zrost[1], T Ferger[1], D Fischer[1], A Dorn[1], J Titze[3], T Jahnke[3], M Schöffler[3], S Schössler[3], T Havermeier[3], M Smolarski[3], K Cole[3], R Dörner[3], T J M Zouros[4], S Düsterer[5], R Treusch[5], M Gensch[5], C D Schröter[1], R Moshammer[1] and J Ullrich[1,2]

[1] Max-Planck-Institut für Kernphysik, 69117 Heidelberg, Germany
[2] Max-Planck Advanced Study Group at CFEL, 22607 Hamburg, Germany
[3] Institut für Kernphysik, Universität Frankfurt, 60486 Frankfurt, Germany
[4] Department of Physics, University of Crete, PO Box 2208, 71003 Heraklion, Crete, Greece
[5] DESY, Notkestrasse 85, 22607 Hamburg, Germany

Received 16 December 2008, in final form 16 January 2009
Published 12 June 2009
Online at stacks.iop.org/JPhysB/42/134012

Abstract
Multiple ionization (MI), induced by a few EUV photons at energies of 28.2 eV, 38 eV and 44 eV from FLASH (the *f*ree-electron *las*er at *H*amburg), has been studied for atoms (He, Ne, Ar) and N_2 molecules utilizing our multi-hit coincident technology—the reaction microscope. At comparably low intensities of $I \cong 10^{11}$–10^{13} W cm^{-2} we find the non-sequential (NS) MI mechanism dominating Ar^{3+} and Ar^{4+} production. Inspecting recoil ion and electron momentum distributions evidence is provided (i) for preferential back-to-back emission of electrons for NS double ionization of He and (ii) for angular entanglement between two outgoing electrons in sequential ionization (SI). In contrast to atoms, SI is observed to be most effective for MI of N_2 molecules at an intensity of $\sim 10^{13}$ W cm^{-2} leading, among others, to $N_2^{2+} \rightarrow N^+ + N^+$, $N_2^{3+} \rightarrow N^{2+} + N^+$, $N_2^{4+} \rightarrow N^{2+} + N^{2+}$ Coulomb explosion channels. Fragment ion momentum distributions are investigated and are demonstrated to allow tracing SI pathways.

(Some figures in this article are in colour only in the electronic version)

1. Introduction

Ultra-brilliant, accelerator-based short-pulse radiation sources of the next generation, such as the free-electron laser (FEL) in Hamburg (FLASH) [1], the only EUV-FEL operational worldwide or the Spring8 Compact SASE Source (SCSS) delivering photons with energies up to 25 eV [2], now open a new chapter for exploring light–matter interactions in so far not accessible regimes. Among them are resonant excitation or ionization of highly charged ions [3], ionization of state prepared molecular ions [4], absorption by mesoscopic nano-particles like clusters (see e.g. [5] and references therein) and, last but not least, basic nonlinear processes where few EUV photons interact with few electrons causing double or multiple ionization of atoms and molecules. FLASH, delivering EUV photons with unprecedented intensities (up to 10^{16} W cm^{-2}) and short pulse durations of 25 fs and less, in combination with the most advanced multi-particle detection systems—the reaction microscope [6]—now opens the door for performing differential experiments in this new regime.

In particular, two-photon double ionization (DI) of He is of fundamental interest since it bridges the gap between the one- and many-photon DI regimes and, thus, is of decisive importance to advance nonlinear theories. Previously, one-photon-induced DI of helium has been central to atomic and molecular physics research at third generation synchrotrons due to its exemplary character to explore electron–electron correlation and is generally considered to be well understood

[7] within the validity of the dipole approximation after decades of research. Many-photon DI of helium as the other extreme, where a couple of ten photons are typically needed using lasers in the visible (800 nm), has until the present day resisted any comprehensive theoretical description due to tremendous complications in solving the nonlinear problem in the non-perturbative regime. Nevertheless, with the availability of differential data since 2000 using the reaction microscope, along with new theory developments at different frontiers, considerable advances have been achieved [8, 9].

Beyond DI, multiple ionization (MI) of atoms by few EUV photons has attracted considerable attention since it represents in general the dominant pathway for the intense EUV pulses to interact with matter. Its understanding is thus of paramount importance for applying FEL pulses in various fields, like cluster or solid-state physics, chemistry and biology. Experimentally, until now, intensity dependences of ion yields have been recorded nearly exclusively revealing, on the basis of perturbation theory, the number of photons that had been needed for creating a certain charge state. This allows us, under certain conditions, to draw conclusions about the dominant ionization mechanisms, sequential or non-sequential (see e.g. [10]). For the photon frequencies at FLASH one safely expects to be in the perturbative regime, surprises have been encountered in these kinds of experiments observing charge states as high as 21 after irradiating Xe atoms with 93 eV photons at 10^{16} W cm^{-2} [11] pointing beyond perturbation theory and causing intense discussions in the community.

Proceeding to molecules, not much is known up to now on multi-photon absorption pathways in the EUV regime. In the recent past, single-photon induced DI and fragmentation of simple molecules like N_2 have been studied extensively since those are among the most relevant interactions occurring in nature of importance for the physics and chemistry of planetary upper atmospheres, of interstellar clouds, for the existence of life and have widespread applications in technical plasmas. With the advent of the new sources, a number of novel possibilities arise. Thus, for example, sequential multi-photon absorption enables one to study the ionization and dissociation dynamics of highly excited and polarized molecular ions that were created in a simple, effective and controlled way by the preceding photons in the same pulse. Here, the first part of the pulse essentially acts as an *in situ*, pulse-synchronized ion source providing a dense, absorption aligned and polarized molecular ion target challenging, e.g. more complex techniques developed for studying EUV interaction with molecular ions like mass-selected ion-beam [4] and fragment-detection methods.

In this contribution, we will first briefly describe the experimental setup, a dedicated reaction microscope developed to explore few-photon MI of atoms and molecules at the new FEL radiation facilities, and then present a series of results in the main part of this paper. In detail, we report differential experimental studies for non-sequential two-photon DI of He at 44 eV and of Ne at 38 eV, as well as for sequential DI of Ne at 44 eV. We then proceed to multiple ionization of argon exploring intensity-dependent ionization yields for Ar^{n+} ($n = 2$, 3 and 4) at $h\nu = 28.2$ eV obtaining the number of photons involved. Finally, first fragment ion momentum distributions (FIMD) are presented for Coulomb explosion after sequential MI of N_2 molecules at 44 eV.

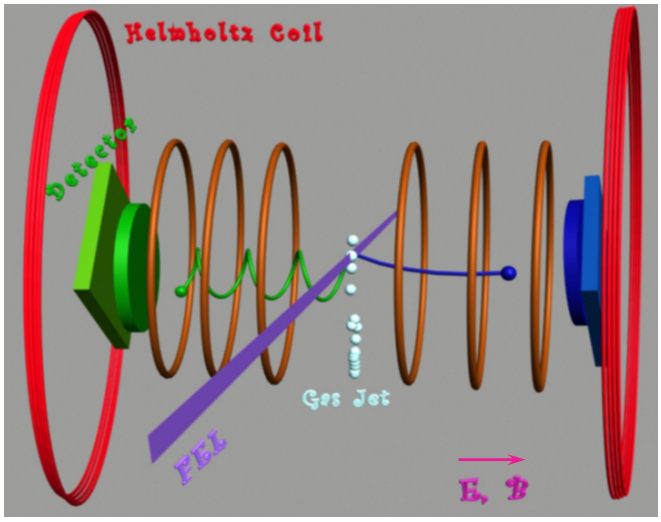

Figure 1. Schematic of a reaction microscope.

2. Experimental setup

The general design of a reaction microscope (REMI) is shown schematically in figure 1. The FEL light, arriving with a variable number of micro-bunches within pulse trains at 5 Hz repetition rate and typical pulse energies of a few up to some tens of μJ, is focused in the interaction chamber reaching peak intensities of $I \cong 10^{11}$–10^{14} W cm^{-2}. Each pulse train used in our experiments consisted of 12 or 24 individual bunches, separated by 10 or 5 μs, respectively. The photon beam then transversally intersects a cold atomic or molecular beam in the centre of the REMI, a supersonic gas jet provided by expanding gas through a nozzle (diameter 30 μm) at a pre-pressure of a few bar and cut via two skimmers (diameters 180 μm and 400 μm, respectively). Four pairs of independently moveable slits are mounted further downstream allowing for additional collimation of the target beam before entering the interaction chamber after four differential pumping stages, such that a well-defined (roughly 0.5 × 0.5 mm in width), dilute ($\cong 10^{10}$ particles cm^{-3}), intrinsically cold ($T_{\rm jet} < 1$ K for atoms and <5 K for molecular ions) supersonic jet is provided and crossed with the focused FEL-beam (about 30 μm in diameter) in the REMI at a base pressure of $\sim 10^{-12}$ mbar. The effective target volume, defined by the overlap of the target jet with the photon beam, is placed in a region where an electrostatic field (normally about 0.5 V cm^{-1} for atoms and 30 ∼ 50 V cm^{-1} for molecules) is applied for the extraction of charged target fragments. Electrons and positive ions are registered on opposite sides of the spectrometer by two large-area position sensitive detectors after passing the acceleration regions (31.4 cm for ions and 20.4 cm for electrons), respectively. The position sensitive detectors used are each consisting of a pair of multi-channel plates (plate diameter 8 cm for electrons and

12 cm for ions) equipped with a delay-line anode for position decoding (position resolution 0.1 mm). The two-layer delay line [12], with each end read out by one of the eight channels of an Acqiris digitizer, allowed us to record the complete wave forms of the four signals [13] and, thus, to resolve in position and time several hits on the detector. Detailed analysis of detected coincidences for molecular fragments showed that the dead time between two subsequent events was about 20 ns. Accordingly, hits in this regime have been neglected in the analysis.

For a few photon-induced MI of atoms in the EUV regime the recoil ions emerge with kinetic energies of some meV or below and extraction fields of a few V cm^{-1} are in general sufficiently high to achieve 4π collection efficiency with the present detector sizes. In the case of Coulomb explosion of molecules induced by few photon absorption the ions can gain larger kinetic energies of even more than 10 eV such that extraction potentials of a couple of tens of V cm^{-1} have to be applied on the spectrometer to ensure a 100% detection solid angle.

Emitted electrons usually have considerably larger kinetic energies making it much harder to collect them by means of electric fields alone. Most of them simply miss the detector under conditions ideally suited for the ion detection. In order to achieve a 4π acceptance together with a good momentum resolution in all three spatial dimensions for electrons (without loosing ideal imaging conditions for the ions), a weak homogeneous magnetic field (about 10 G), generated by a pair of large Helmholtz coils, is additionally superimposed along the spectrometer axis effectively confining the electron motion transverse to the extraction direction along the electric field. From the measured time-of-flight (TOF) and position of impact on the detector of each individual particle the initial three-dimensional momentum vectors can be reconstructed on the basis of five time signals, one taken from the voltage contact ring of the multi-channel plate (TOF) and four from the respective connections of the delay-line anode (position). Typically, electron and ion momentum resolutions as good as 0.05 a.u. and 0.3 a.u., respectively, have been achieved so far at FLASH extracted by inspecting sum-momentum peak width under momentum conservation conditions for single ionization of He.

A typical ion TOF spectrum for multi-charged Ar^{n+} ($n = 1, \ldots, 4$) is presented in figure 2. The momentum component along the extraction field is contained in the width of the peaks; the position spectrum yields the remaining two momentum components. Due to our excellent background pressure the spectrum is widely free of background such that even small peaks can be clearly identified. On the basis of the well-known cross sections for single-photon single, double, and triple ionization of Ar by synchrotron radiation [14, 15], one can estimate the relative intensity of different charge states as compared to singly charged ions that would result from single-photon ionization from the FEL third harmonic radiation to be at least one order of magnitude lower than present experimental results. This provides evidence that the observed multi-charged ions result mainly from few-photon ionization which was previously confirmed for MI of Ne at 38 eV [10].

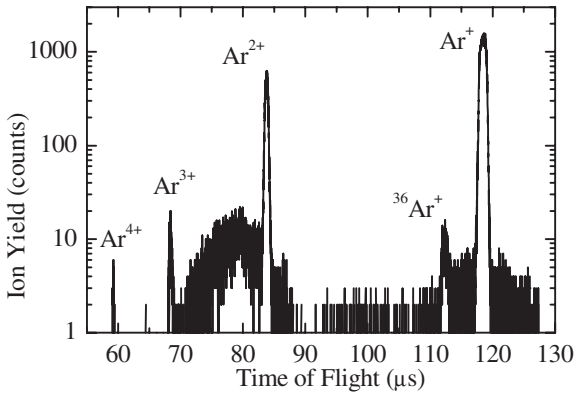

Figure 2. Time-of-flight mass spectra of Ar$^{(1-4)+}$ ions at $I = 2 \times 10^{11} - 4 \times 10^{12}$ W cm^{-2}.

Pulse-to-pulse energy information was obtained by recording the current on a metal plate induced by each individual FLASH pulse. Comparing the average current over several thousand pulses with the mean pulse energy provided by an energy profiler in the machine, the absolute energy of each pulse could be deduced. On the basis of this number, the approximately known focal spot size (30 μm diameter), and the pulse duration ($\sim$30 fs), the light intensities were calculated with an estimated uncertainty of a factor of 5.

3. Results

3.1. Recoil-ion momentum distributions for direct two-photon DI of He

Two-photon DI has become a benchmark system for exploring electron–electron correlation in the nonlinear EUV regime. Two different pathways are usually distinguished in the calculations, 'sequential' or 'non-sequential' (direct) ionization, with one or the other dominating two-electron ejection depending on the photon energy and intensity. Whereas non-sequential ionization (NSI) requires that two electrons are ionized by 'simultaneous' absorption of two photons through virtual intermediate states, sequential ionization (SI) proceeds through a stationary real intermediate state of the ion via 'time-sequenced' absorption of two photons within the same light pulse from FLASH. Due to its simultaneous rather than 'step-by-step' character two-photon NSI provides a much richer setting for the photon–electron interaction as well as for electron–electron correlation mechanisms.

Theoretically, as was mentioned before, the application of perturbative methods is fully justified at not too high intensities (less than 10^{15} W cm^{-2}) since here, the quiver energy of a free electron in the electromagnetic field, scaling with $1/\omega^2$ (with ω being light frequency), is negligibly small compared to the atomic binding potential as well as to the energy transferred by two-photon absorption. This, along with the fact that only two photons and two electrons are involved, nurtures the hope for having rigorous theoretical calculations at hand. Instead and most surprising however, present state-of-the-art theories, most of them sophisticated numerical solutions

of the time-dependent Schrödinger equation, differ even in the prediction of the total cross section by up to a factor of 10 despite enormous recent efforts within the last two years [16–19].

At the experimental front, doubly charged He ions resulting from two-photon absorption using 42 eV high-harmonic radiations were first observed by Nabekawa [20]. Subsequently, intensity-dependent experiments [21] yielding total cross sections and pioneering differential studies (recoil-ion) of two-photon DI in He [22] and Ne [10] were performed at FLASH. First, fully differential measurements investigated sequential two-photon DI of Ne at a photon energy of 44 eV [23]. Here, the emission angles of the two outgoing electrons were found to be correlated via the polarized Ne^+ intermediate state which agrees well with theoretical predictions [24, 25], indicating that even SI might be not as simple as expected.

In figure 3, we compare the recoil-ion momentum distributions for double ionization of He via single-photon absorption at 99 eV (a) [26], two-photon ionization at 44 eV (b) and, finally, multi-photon absorption of 1.5 eV photons from a Ti:Sa laser (c) [26]. Distinct differences are observed and might be traced back to different dynamical mechanisms being at work [26]. Since the He^{2+} ion momentum compensates the sum momentum of both outgoing electrons it contains information about their angular and energy correlation. For single-photon absorption, one finds a clear dipolar pattern that can be explained by the fact that the photon is initially absorbed by one of the He electrons, causing a distinct nuclear recoil which is only little disturbed by the subsequent electron–electron interaction leading to double ionization. The minimum of the ion momentum distribution at $P_z = 0$ is also a consequence of the $^1P^o$ symmetry of the two-electron final state. This symmetry prohibits most of the electron angular configurations which lead to zero momentum of the ion in polarization direction. Even though the momentum distribution looks quite similar for multi-photon DI in figure 3(c), the reasons for this pattern are significantly different. Here, the first electron tunnel in the strong optical field, not perturbative due to its low frequency, is then driven by the field and occasionally re-collides with the parent ion emitting the second electron in an ionizing collision. Since this encounter occurs close to the minimum of the time-dependent electric field of the laser, the corresponding drift momentum of the He^{2+} ion observed in the final state is large, leading to the two maxima.

In the pattern observed for two-photon DI (in figure 3(b)), we find an essentially unstructured distribution peaking at the origin. Since the first and second ionization potentials for He are 24.5 eV and 54.4 eV, respectively and, thus, a minimum energy of 79 eV is needed to doubly ionize the He atoms, at least two photons have to be simultaneously absorbed for photon energies between 40 and 54 eV. Sequential ionization is only feasible for photon energies equal or beyond 54 eV and we can safely exclude SI at 44 eV. In principle, three-photon DI of He could occur, where the first step is sequential and the second one would be direct 'above-threshold' two-photon absorption from the He^+ ground state. However, at the present photon energy NSI is theoretically [27] predicted to dominate

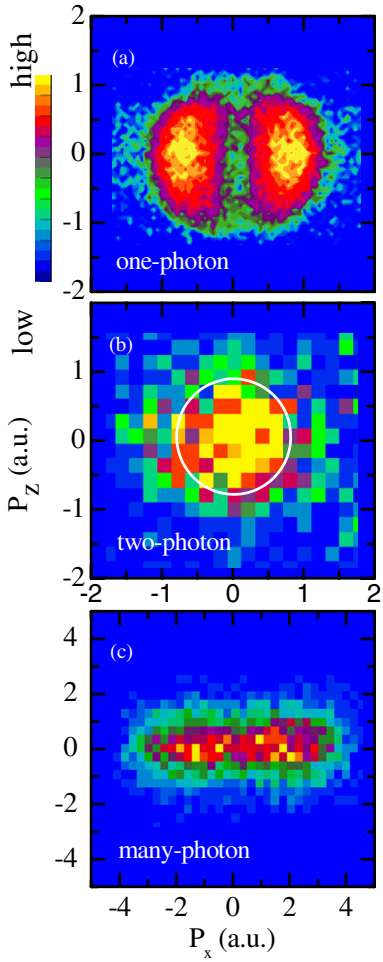

Figure 3. Density plot of recoil-ion momentum distributions for He^{2+} ions created via one-photon absorption at 99 eV (a) (taken from [26]), two-photon absorption at 44 eV (b) and many-photon absorption at 1.5 eV from a Ti:Sa laser (c) (taken from [26]). The solid curve in (b) indicates the positions of maximum momenta for the case, in which two electrons are ejected into the same direction after the simultaneous absorption of two photons. The polarization of the light, the propagation of the light and time-of-flight direction of fragments are marked as *x*-, *y*- and *z*-directions, respectively. The events in the *y*-direction are integrated in this plot.

at low intensities $I < 10^{15}$ W cm^{-2} which was confirmed experimentally on the basis of the He^{2+} yield depending quadratically on the light intensity at a photon energy of 42 eV [20] as well at 42.8 eV [21]. Also, the possible enhancement of SI which might occur if the second photon exactly hits excited ionic states such as He^+ (2p) and He^+ (3p) (40.8 eV and 48.4 eV relative to He^+ (1 s)) can be excluded at the present photon energy of 44 eV.

Indicated as a circle in figure 3(b) with a radius of 0.81 a.u. is the location of the maximum momentum the recoiling ion could acquire when two electrons are ejected into the same direction with equal momenta, a scenario that was predicted in early calculations. Instead, most of them lie well within the circle such that we can conclude that the two electrons preferentially emerge into opposite hemispheres with similar energies for two-photon NSDI of He in striking contrast to the dynamics of one-photon DI (figure 3(a)), where exact

back-to-back emission along the polarization direction is forbidden by the dipole selection rules [28, 29]. The present recoil-ion momentum distributions are in qualitative agreement with recent theoretical predictions [17, 30]. However, we also note that two shoulders do appear along the polarization (around $P_x \cong \pm 0.5$ a.u.) in some of the predictions, not observed in the experiment. This could be due to insufficient statistical significance of the present measurement such that further investigations are required.

Beyond He, experimental [21] and theoretical studies [31, 32] have started to investigate more complicated atoms like Ne, again usually reporting total cross sections mostly not allowing one to draw definite conclusions concerning the physical mechanisms underlying two-electron ionization dynamics. The recoil-ion momentum distribution given in [10] presented the DI of Ne at 38 eV for a rather low intensity of 10^{12} W cm^{-2} where most of the events again lie well within the circle of radius of 1.05 a.u., equivalent to figure 3(b). Thus, along the same arguments as above, we find the two electrons primarily compensating their momentum, pointing to a dominant NSI.

3.2. Fully differential measurements for sequential two-photon DI of Ne at 44 eV

At a photon energy of 44 eV, Ne^{2+} can be created by the sequential absorption of two photons within one light pulse, illustrated in figure 4 by inspecting the respective ionization potentials. Here, SI might proceed via one of the intermediate ionic states of Ne^+ populated by absorption of the first photon by the Ne atom in the ground state. From the ionization potentials one would expect that the electron from the first ionization step is centred at an energy of about 22.4 eV. The second electron then either emerges with a kinetic energy of about 3 eV, or just very close to zero energy, indicating that the Ne^{2+} ion is left in the ^{3}P state or in the ^{1}D state, respectively. In a recent experiment, both electrons with distinguishable energies were detected in coincidence with the Ne^{2+} recoil ion for the first time.

Momentum distributions of Ne^{2+} ions and of the outgoing electrons are displayed in figures 5(a) and (b), respectively. In contrast to recoil ions for non-sequential two-photon DI of Ne at 38 eV in [10] and He at 44 eV shown in figure 3(b) the emission characteristics of Ne^{2+} ions at 44 eV exhibits significant changes. Here, a dipole-like structure appears instead of an accumulation of most events for NSI at the origin. This provides first and clear kinematical evidence for another ionization mechanism, namely SI to dominate. Moreover, the dipole-like pattern parallel to the polarization direction indicates positive values for the asymmetry parameter β_2 for the 'first' electron emitted at higher energies and, thus, dominating the ion recoil as indicated by the full line. The observed structure is quite broad, which is straightforward to interpret as being due to the momentum of the second electron emitted from the ion thereby just adding its momentum to the ion equally likely along all spatial directions, in first approximation. Two further broken-line circles in the figure mark the maximum and minimum sum momentum expected

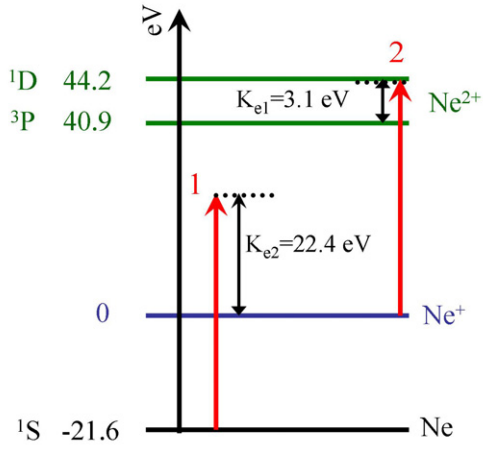

Figure 4. Schematic for relevant energy levels of Ne, Ne^+ and Ne^{2+}. The two vertical lines marked 1 and 2 represent possible transition processes induced by absorption of the first and second photons, respectively.

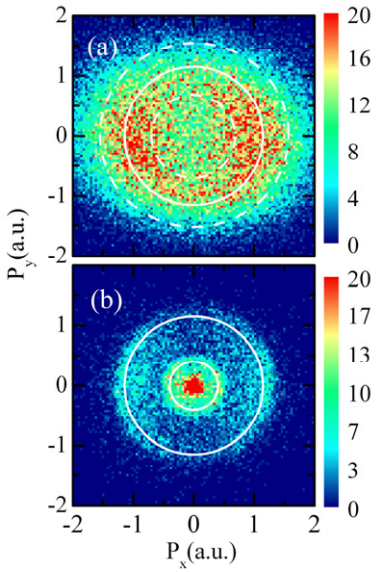

Figure 5. Momentum distributions of Ne^{2+} recoil-ions (a) and of two electrons in coincidence (b), which are created at a photon energy of 44 eV leading to SI ionization. Directions are the same as in figure 3.

by adding or subtracting both electron momenta in one plane.

Figure 5(b) depicts the momentum distribution of coincident electrons, and two circles are clearly visible in addition to a peak occurring at the origin. While the outer ring corresponds to electrons with kinetic energies of 22.5 eV (the first ionized electron) the inner one is due to the 3 eV electrons, i.e. of the second electron leaving the remaining Ne^{2+} ion in the ^{3}P state. In the centre we find electrons with almost zero kinetic energy, resembling ions being left in the ^{1}D final state. Whereas the fastest electrons clearly display a dominant emission along the light polarization direction in qualitative agreement with that of the recoiling ion in figure 5(a), the second electron, is found to be more isotropically distributed. This is surprising at first glance, since such

a behaviour would not be expected for photo-ionization of unpolarized Ne^+ ions emerging from any kind of independent ion source. Thus, we find evidence that the two electrons are correlated via the intermediately populated and polarized Ne^+ state as recently predicted theoretically [25]. There it was shown that even the angular emission characteristics of the first electron depends on the ejection angle of the second such that it 'knows' whether or not the second electron is ionized questioning the simple picture of a 'stepwise', time-sequenced, sequential ionization and possibly pointing to an angular-entanglement of both electrons. This will be investigated in more detail experimentally in a forthcoming paper [23].

3.3. Multiple ionization of Ar at hv = 28.2 eV

Few experiments on EUV multi-photon ionization of Ar have been reported so far. At 98 nm Wabnitz *et al* [33] studied MI of Ar at FLASH and recently Benis *et al* [34] observed two-photon DI of Ar by a superposition of harmonics. Again at FLASH with 38 eV photons, we have studied before MI of Ar [10] observing charge states up to Ar^{3+} created by the absorption of three or four photons, which indicated a mixture between SI (four photons required) and NSI where only two photons are needed.

In general, since NSI proceeds through intermediate virtual states and SI is approximated as a 'stepwise' absorption (see, e.g., [10]) involving intermediate stationary levels, typically more photons are required for SI to reach the same final charge state as for NSI. Moreover, as the ionization yield should increase with the light intensity as $Y = \sigma_n I^n$ according to perturbation theory, where I is the intensity, σ_n is the generalized n-photon cross section and n is the number of involved photons, NSI is predicted to dominate at low intensities, whereas the sequential mechanism takes over at higher ones [31]. Thus, proceeding to lower intensities we might expect pure non-sequential ionization to mainly contribute to Ar multiple ionization, which can be proven in certain cases by measuring the ion yields for various channels as a function of the intensity and, thereby, 'counting' the number of absorbed photons (see e.g. [10]).

Along these lines we have investigated MI of Ar at low intensities and photon energy of 28.2 eV. This implies that for NSI two, three and six photons are required for the creation of Ar^{2+}, Ar^{3+} and Ar^{4+}, respectively, whereas two, four and seven photons are needed for SI (see the inset in figure 6). The $Ar^{(2-4)+}$ yields are analysed as a function of intensities I in figure 6. The fits nicely describe the ion-yield intensity dependences with the slopes $n = 2.0 \pm 0.1$, 3.1 ± 0.4, 5.3 ± 1.0, respectively. This indicates that triple and quadruple ionizations of Ar are now induced essentially via NSI, different from our previous results [10] at 38 eV, where NSI as well as SI was observed to contribute to Ar^{3+}. As mentioned above, such a behaviour might be expected for the present pulse intensities [31] being about one order of magnitude lower than in previous measurement [10] demonstrating that by carefully selecting photon energies and laser intensities, along with a widely background-free detection of the ions allows one to unambiguously identify the MI ionization mechanism

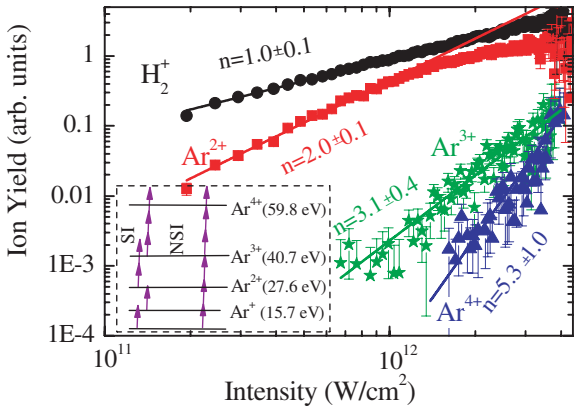

Figure 6. Ion yield of $Ar^{(1-4)+}$ and H_2^+ as a function of the light intensities I in a double logarithmic representation. An energy scheme relevant for multiple ionization of Ar is plotted in the inset. The number of arrows indicates the photon numbers absorbed from the initial state to the respective ionic states. The numbers in parenthesis are the first four ionization potentials of Ar. Solid symbols and solid lines denote the present measurements and fits ($\log Y = n \log I + \log \sigma_n$), respectively.

for special cases. Note that the present observations are in agreement with the dominant non-sequential DI of Ne found at relative low intensities of $\cong 10^{12}$ W cm^{-2} in [10]. Certainly, however, we cannot distinguish SI and NSI for DI of Ar on the basis of ion-yield dependences alone, since both require the absorption of two photons. Here, differential experiments would be needed as shown before to discriminate between both mechanisms which were not feasible, however, in the present measurement since the ion-momentum resolution for the heavy Ar ions was not sufficient.

3.4. Few photon-induced multiple ionization of N_2

We finally proceed to discuss some aspects of MI for an even more complex target, namely the N_2 molecule. In this paper, we only present first results and provide a qualitative interpretation. A detailed analysis will be the subject of a forthcoming dedicated publication [35]. The nitrogen molecule was chosen since it has been investigated previously in great detail, theoretically as well as experimentally. A wealth of results has been reported for EUV single-photon interactions [36–43], intense laser impact [44, 45] including time-dependent studies [46], and high-resolution electron impact coincidence measurements [47]. Recently, MI of N_2 induced by few EUV photons was studied on the level of total cross sections [48, 49] or providing time-of-flight spectra of ions [50].

A photo-ion–photo-ion-coincidence (PIPICO) TOF spectrum measured at a photon energy of 44 eV is displayed in figure 7. Three Coulomb explosion reactions $N_2^{2+} \rightarrow N^+ + N^+$, $N_2^{3+} \rightarrow N^{2+} + N^+$ and $N_2^{4+} \rightarrow N^{2+} + N^{2+}$ are clearly identified as hyperbolic lines. On the basis of intensity-dependent coincident $N^+ + N^+$ yields, we judge that those are created by sequential absorption of two photons via intermediate ionic states, e.g. via bound N_2^+ states or the F- and H-bands of N_2^+, populated effectively by the first photon [35]. Similarly, as much as five photons were found to be absorbed for the

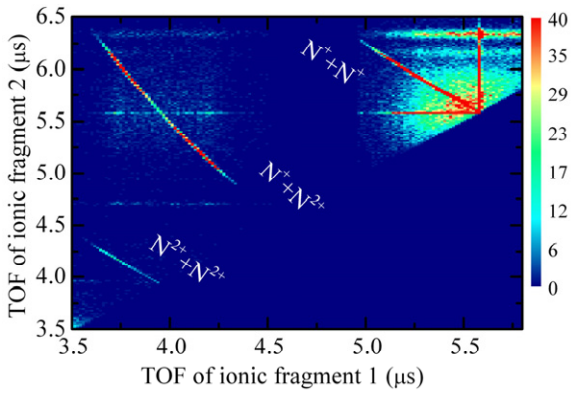

Figure 7. PIPICO-TOF spectra. The time-of-flight of one ion is plotted versus the time-of-flight of the second.

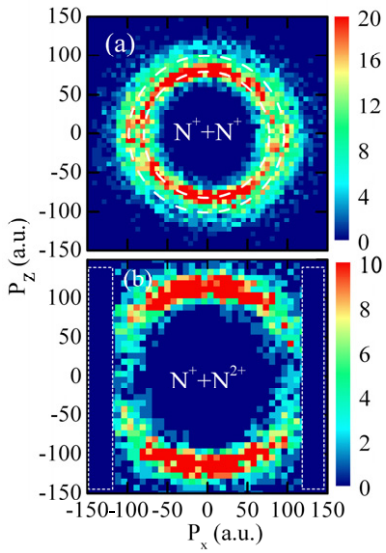

Figure 8. FIMD density plots for fragmentation channels $N_2^{2+} \rightarrow N^+ + N^+$ (a) and $N_2^{3+} \rightarrow N^{2+} + N^+$ (b). The two circles in (a) indicate dissociating $A^1\Pi_u$ and $d^3\Pi_g$ states (the inner circle) and the $D^1\Sigma_u$ state (the outer circle). Dotted lines in (b) mark inaccessible areas due to the limited angular acceptance of the ion detector. The events plotted in both (a) and (b) are integrated for $|P_z| < 30$ a.u.

creation of intermediate N_2^{3+} ions, even though already two would be enough (via NSI) relying on the potential curves given by Bandrauk [51].

In general we have found, and this is the first important conclusion for MI of molecules, that SI dominates at 44 eV photon energies for essentially all multiple ionization, dissociation and Coulomb explosion channels investigated. This result might be expected due to the fact, that a molecule offers a large number of intermediate stationary or quasi-stationary states such that SI 'always' finds a suitable intermediate step to further absorb photons making this mechanism most effective. This suggests that SI is the dominant process at other EUV wavelengths as well. In our specific case it is completely unclear, however, why for certain channels the number of photons significantly exceeds the minimum number required. Thus, the creation of the N_2^{3+} intermediate state by five photons means an excess of three photons as compared to the NSI and still of two relative to the lowest-energetic SI channel. Due to the absence of photo-electron spectra this question cannot be clarified in the present experiment.

In order to further elucidate MI dynamics in intense EUV fields we present two-dimensional fragment ion momentum distributions for two Coulomb explosion channels, $N^+ + N^+$ and $N^+ + N^{2+}$, in figures 8(a) and (b). Due to the quite short dissociation times of most of the intermediate and final states involved for these two channels, typically below 100 fs (with the exception of some meta-stable levels) as compared to the typical rotation period of ∼10 ps, the direction of motion for the ionic fragments directly reflects the spatial alignment of the parent molecular ions at the instant of photo-ionization (axial recoil approximation [52]). Therefore, measuring three-dimensional fragment ion momentum distributions allows one to investigate in detail the dynamics of photo-absorption, the potentially preferred absorption of molecules aligned along a certain direction with respect to the photon polarization axes and, thus, the alignment of molecular ions produced via photo-absorption from a randomly oriented ensemble of molecules.

One first clearly observes in figure 8(a) for $(N^+ + N^+)$-explosion, that different channels, identified by their kinetic energy releases (KER, circles with certain radii in the two-dimensional momentum plot) show vastly different angular distributions. Thus, $A^1\Pi_u$ and $d^3\Pi_g$ states, the inner circle with small KERs (not separated due to the integration of a large interval along P_z), fragment perpendicular to the polarization direction $\hat{\varepsilon}$ whereas the $D^1\Sigma_u$ states tend to emerge along $\hat{\varepsilon}$ (note that part of the final-state fragment phase space along the polarization direction cannot be fully recorded due to the detector dead time for fragments with the same charge-to-mass ratio exhibiting identical TOFs in this configuration). Since two photons have been absorbed in this channel along with the fact that the molecule cannot rotate within the ∼25 fs FEL pulse this leads directly to the conclusion that different final $(N^+ + N^+)$ states are dominantly populated through different N_2^+ intermediate states, with different alignment and polarization properties created by the absorption of one photon in the first step.

This is further elucidated by inspecting the $(N^{2+} + N^+)$ channel in figure 8(b) where the full final phase space is accessible due to the different charge-to-mass ratio of the two fragments. Here, one finds predominant emission perpendicular to $\hat{\varepsilon}$ which immediately rules out, e.g. the $N_2^{2+}\left(D^1\Sigma_u^+\right) \rightarrow N^+ + N^+$ state as intermediate sequential step along the arguments given above.

In summary, similarly as discussed in the case of sequential ionization of Ne, we most effectively produce *in situ* and 'just in time' on a ∼30 fs time scale a polarized, aligned and dense molecular ion target that then is investigated via photo-absorption in one of the subsequent steps of SI. We would like to emphasize that the intermediate molecular ion state can be fully identified by choosing the photon energy or measuring the emerging photo-electron energies (and emission angles) which is straightforward in future exploitation of the

full capabilities of the REMI. This would not only open the door to completely trace SI pathways, only partially demonstrated in the present pioneering work, but, moreover, allow us to investigate highly excited states of molecules and, practically inaccessible up to now, of molecular ions.

4. Conclusions

Multiple ionization of atoms (He, Ne and Ar) and of the N_2 molecule, induced by the absorption of a few EUV photons per atom/molecule from the FLASH has been studied on various levels of sophistication using a dedicated reaction microscope. Starting by simply inspecting the intensity-dependent ion yields for Ar^{3+} and Ar^{4+} production by 28.2 eV photons the dominance of non-sequential ionization at low intensities with up to six photons being absorbed was unambiguously revealed. Proceeding to differential cross sections, recoil-ion momentum distributions for He^{2+} and Ne^{2+} were investigated for non-sequential absorption of two photons. It was found that most of the events exhibited small momenta, with the distribution peaked at zero, pointing to the dominance of back-to-back emission of the two electrons preferentially sharing comparable excess energies. In a further step, we confirmed SI leading to a dipole-like structure in the Ne^{2+} recoil-ion momentum distributions for DI of Ne at 44 eV. Here we have performed a fully differential experiment, detecting the ion and two electrons in coincidence, thus finding evidence for angular correlation between the two electrons that are correlated or possibly even entangled through the polarized intermediate state, indicating, as a result, that SI might be not as simple as expected. Finally, differential studies for MI of the N_2 molecule demonstrate the effectiveness of sequential ionization due to the rich structure of excited and ionic molecular states involved. Coincident momentum distributions for the $N^+ + N^+$ and $N^+ + N^{2+}$ Coulomb explosion channels allowed us to draw some first conclusions about SI pathways.

The present results provide first information on the dynamics of MI induced by EUV photons, stimulating the development of advanced theoretical methods and start to shed light on the nonlinear interaction of light with matter in this new wavelength regime. In a recent beam time in December 2008, we were able to successfully commission a split-mirror delay stage and recorded first time-dependent data for dissociating N_2^{n+} molecules, pointing to the rich future potential of the field, especially as the investigation of highly excited molecular states is concerned.

Acknowledgments

Support from the Max-Planck-Advanced Study Group at the Center of Free-Electron Laser Science (CFEL) and from HGF 'Virtual Institut Atomic and Cluster Physics at FEL' is gratefully acknowledged. YHJ thanks for support from DFG project no JI 110/2-1. We are greatly indebted to the scientific and technical team at FLASH, in particular the machine operators and run coordinators, all together being the foundation of its outstanding performance.

References

[1] Ackermann W *et al* 2007 *Nat. Photonics* **1** 336
[2] Shintake T *et al* 2008 *Nat. Photonics* **2** 555
[3] Epp S W *et al* 2007 *Phys. Rev. Lett.* **98** 183001
[4] Pedersen H B *et al* 2007 *Phys. Rev. Lett.* **98** 223202
[5] Bostedt C *et al* 2008 *Phys. Rev. Lett.* **100** 133401
[6] Ullrich J, Moshammer R, Dorn A, Dörner A, Schmidt L and Schmidt-Böcking H 2003 *Rep. Prog. Phys.* **66** 1463
[7] Briggs J S and Schmidt V 2000 *J. Phys. B: At. Mol. Opt. Phys.* **33** R1
[8] Becker A, Dörner R and Moshammer R 2005 *J. Phys. B: At. Mol. Opt. Phys.* **38** S753
[9] Dörner R *et al* 2002 *Adv. At. Mol. Phys.* **48** 1
[10] Moshammer R *et al* 2007 *Phys. Rev. Lett.* **98** 203001
[11] Sorokin A A *et al* 2007 *Phys. Rev. Lett.* **99** 213002
[12] Jagutzki O *et al* 2002 *Nucl. Instrum. Methods Phys. Res.* A **477** 244–9
[13] Foucar L 2008 *Dissertation* Universität Frankfurt http://rds1.atom.uni-frankfurt.de/web/publications/files/Lutz_Foucar_2008.pdf
[14] Holland D M P, Coding K, West J B and Marr G V 1979 *J. Phys. B: At. Mol. Opt. Phys.* **12** 2465
[15] Marr G V and West J B 1976 *At. Data Nucl. Data Tables* **18** 497
[16] Nikolopoulos L A A and Lambropoulos P 2007 *J. Phys. B: At. Mol. Opt. Phys.* **40** 1347
[17] Foumouo E, Antoine Ph, Piraux B, Malegat L, Bachau H and Shakeshaft R 2008 *J. Phys. B: At. Mol. Opt. Phys.* **41** 051001
[18] Feist J, Nagele S, Pazourek R, Persson E, Schneider B I, Collins L A and Burgdörfer J 2008 *Phys. Rev.* A **77** 043420
[19] Guan X, Bartschat C and Schneider B I 2008 *Phys. Rev.* A **77** 043421
[20] Nabekawa Y, Hasegawa H, Takahashi E J and Midorikawa K 2005 *Phys. Rev. Lett.* **94** 043001
[21] Sorokin A A, Wellhöfer M, Bobashev S V, Tiedtke K and Richter M 2007 *Phys. Rev.* A **75** 051402
[22] Rudenko A *et al* 2008 *Phys. Rev. Lett.* **101** 073003
[23] Kurka M *et al* 2008 *Phys. Rev. Lett.* (submitted)
[24] Kheifets A 2007 *J. Phys. B: At. Mol. Opt. Phys.* **40** F313
[25] Fritzsche S, Grum-Grzhimailo A N and Kabachnik N M 2008 *J. Phys. B: At. Mol. Opt. Phys.* **41** 165601
[26] Weber Th *et al* 2001 *Opt. Express* **8** 368
[27] Nikolopoulos L A A and Lambropoulos P 2006 *J. Phys. B: At. Mol. Opt. Phys.* **39** 883
[28] Knapp A *et al* 2002 *J. Phys. B: At. Mol. Opt. Phys.* **35** L521
[29] Huetz A and Mazeau J 2000 *Phys. Rev. Lett.* **85** 530
[30] Horner D A, Rescigno T N and McCurdy C W 2008 *Phys. Rev.* A **77** 030703
Horner D A, McCurdy C W and Rescigno T N 2008 *Phys. Rev.* A **78** 043416
[31] Makris M G and Lambropoulos P 2008 *Phys. Rev.* A **77** 023401
[32] Hamonou L and Van Der Hart H W 2008 *J. Phys. B: At. Mol. Opt. Phys.* **41** 121001
[33] Wabnitz H *et al* 2005 *Phys. Rev. Lett.* **94** 023001
[34] Benis E P *et al* 2006 *Phys. Rev.* A **74** 051402
[35] Jiang Y H *et al* 2008 *Phys. Rev. Lett.* (submitted)
[36] Gisselbrecht M *et al* 2006 *Phys. Rev. Lett.* **96** 153002
[37] Reddish T J *et al* 2008 *Phys. Rev. Lett.* **100** 193001
[38] Besnard M J, Hellner L, Dujardin G and Winkoun D 1988 *J. Chem. Phys.* **88** 1732
[39] Franceschi P, Ascenzi D, Tosi P, Thissen R and Zabka J 2007 *J. Chem. Phys.* **126** 134310
[40] Weber Th *et al* 2001 *J. Phys. B* **34** 3669
[41] Rolles D *et al* 2005 *Nature* **437** 711
[42] Schöffler M S *et al* 2008 *Science* **320** 920

[43] Zimmermann B *et al* 2008 *Nat. Phys.* **4** 649
[44] Hishikawa A *et al* 1998 *Chem. Phys.* **231** 315
[45] Voss S *et al* 2004 *J. Phys. B: At. Mol. Opt. Phys.* **37** 4239
[46] Gagnon E *et al* 2007 *Science* **317** 1374
[47] Lundqvist M, Edvardsson D, Baltzer P and Wannberg B 1996 *J. Phys. B: At. Mol. Opt. Phys.* **29** 1489
[48] Sorokin A A, Bobashev S V, Tiedtke K and Richter M 2006 *J. Phys. B: At. Mol. Opt. Phys.* **39** L299
[49] Föhlisch A *et al* 2007 *Phys. Rev.* A **76** 013411
[50] Sato T *et al* 2008 *Appl. Phys. Lett.* **92** 154103
[51] Bandrauk A D, Musaev D G and Morokuma K 1999 *Phys. Rev.* A **59** 4309
[52] Zare R N 1972 *Mol. Photochem.* **4** 1